

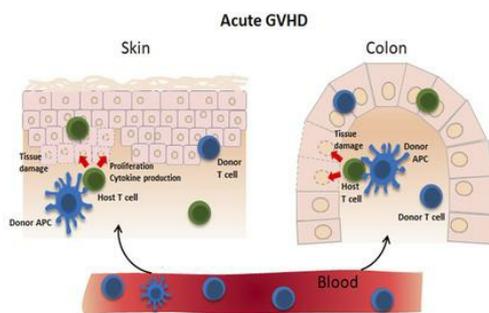
Peripheral host T cells survive hematopoietic stem cell transplantation and promote graft-versus-host-disease

Sherrie J. Divito, ... , Frode L. Jahnsen, Thomas S. Kupper

J Clin Invest. 2020. <https://doi.org/10.1172/JCI129965>.

Research In-Press Preview Immunology

Graphical abstract



Find the latest version:

<https://jci.me/129965/pdf>



1 **Title: Peripheral host T cells survive hematopoietic stem cell transplantation and promote graft-versus-host-**
2 **disease**

3
4 **Authors:**

5 Sherrie J. Divito MD,PhD^{1*}, Anders T. Aasebø MD^{2*}, Tiago R. Matos^{1*}, Pei-Chen Hsieh BS¹, Matthew Collin, MD,
6 PhD³, Christopher P. Elco MD,PhD⁴, John T. O'Malley MD,PhD¹, Espen S. Bækkevold PhD², Henrik Reims MD,PhD⁵,
7 Tobias Gedde-Dahl MD,PhD⁶, Michael Hagerstrom BS⁷, Jude Hilaire BS⁷, John W. Lian¹, Edgar L. Milford MD⁸,
8 Geraldine S. Pinkus, MD⁷, Vincent T. Ho MD⁹, Robert J. Soiffer MD⁹, Haesook T. Kim PhD¹⁰, Martin C. Mihm MD¹,
9 Jerome Ritz MD⁹, Indira Guleria PhD⁸, Corey S. Cutler MD⁹, Rachael A. Clark MD,PhD^{1^}, Frode L. Jahnsen MD,PhD^{2^},
10 Thomas S. Kupper MD^{1^}

11
12 *These authors share the first-author position. Each of the three first authors contributed key data to the overall
13 manuscript. The order was determined based on degree of work contributed both in the laboratory and in preparation of
14 the manuscript with S.J. Divito contributing the most, then A.T. Aasebo, then T.R. Matos.

15
16 ^These authors share senior authorship.

17
18 **Affiliations:**

- 19 1. Department of Dermatology, Brigham and Women's Hospital, Boston, MA, USA 02115
 - 20 2. Department of Pathology, University of Oslo and Oslo University Hospital - Rikshospitalet, 0424 Oslo, Norway
 - 21 3. Newcastle University and NIHR Newcastle Biomedical Research Centre at Newcastle upon Tyne Hospitals NHS
22 Foundation Trust, Newcastle upon Tyne, NE2 4HH, UK
 - 23 4. Department of Pathology and Laboratory Medicine, Brown University, Providence, RI, USA 02912
 - 24 5. Department of Pathology, Oslo University Hospital - Rikshospitalet, 0424 Oslo, Norway
 - 25 6. Department of Hematology, Institute of Clinical Medicine, University of Oslo and Oslo University Hospital -
26 Rikshospitalet, 0424 Oslo, Norway
 - 27 7. Department of Pathology, Brigham and Women's Hospital, Boston, MA, USA 02115.
 - 28 8. Renal Transplant Program, Division of Renal Medicine, Brigham and Women's Hospital, Boston, MA, USA
29 02115.
 - 30 9. Division of Hematological Malignancies and Stem Cell Transplantation, Dana-Farber Cancer Institute, Boston,
31 MA, USA 02215
 - 32 10. Biostatistics and Computational Biology, Dana-Farber Cancer Institute, Boston, MA, USA 02215
- 33

34 **^Corresponding Authors:**

35
36 Thomas S. Kupper
37 Harvard Institutes of Medicine, Rm 673
38 77 Avenue Louis Pasteur
39 Boston, MA 02115
40 Phone 617-525-5550
41 Fax 617-525-5571
42 tkupper@bwh.harvard.edu

43
44 Frode L. Jahnsen
45 A3.M023
46 Department of Pathology
47 Sognavnsveien 20
48 Rikshospitalet
49 0372 Oslo
50 Phone +47 23071444

51 f.l.jahnsen@medisin.uio.no
52
53 Rachael A. Clark
54 EBRC Room 505A
55 221 Longwood Ave
56 Boston, MA 02115
57 Phone 617-962-3386
58 rclark@bwh.harvard.edu

59

60 Conflict of Interest Statement: The authors have declared that no conflict of interest exists.

61 **Abstract**

62 Graft-versus-host-disease (GVHD) is a major cause of morbidity and mortality in hematopoietic stem cell transplantation
63 (HSCT). Donor T cells are key mediators in pathogenesis but a contribution from host T cells has not been explored, as
64 conditioning regimens are believed to deplete host T cells. To evaluate a potential role for host T cells in GVHD, the
65 origin of skin and blood T cells was assessed prospectively in patients after HSCT in the absence of GVHD. While blood
66 contained primarily donor-derived T cells, most T cells in the skin were host-derived. We next examined patient skin,
67 colon and blood during acute GVHD. Host T cells were present in all skin and colon acute GVHD specimens studied yet
68 were largely absent in blood. We observed acute skin GVHD in the presence of 100% host T cells. Analysis demonstrated
69 that a subset of host T cells in peripheral tissues were proliferating (Ki67⁺) and producing the pro-inflammatory cytokines
70 IFN γ and IL-17 in situ. Comparatively, the majority of antigen presenting cells (APC) in tissue in acute GVHD were
71 donor-derived, and donor-derived APC were observed directly adjacent to host T cells. A humanized mouse model
72 demonstrated that host skin-resident T cells could be activated by donor monocytes to generate a GVHD-like dermatitis.
73 Thus, host tissue-resident T cells may play a previously unappreciated pathogenic role in acute GVHD.

74

75 **Introduction**

76 Graft-versus-host disease (GVHD) is a major cause of morbidity and mortality in hematopoietic stem cell transplantation
77 (HSCT) (1-6). Current dogma holds that donor T cells, either transferred with or arising from the donor stem cell product,
78 are activated in the setting of the inflammatory milieu generated by HSCT conditioning and mediate GVHD by damaging
79 host tissues (reviewed in (7, 8)). Pre-transplant conditioning regimens consist of one or more chemoimmunotherapeutic
80 drugs, sometimes with total body irradiation, that are administered to patients prior to donor cell infusion. The goal is to
81 reduce tumor load, provide physical space in host bone marrow to allow engraftment, and prevent host-mediated graft
82 rejection by depleting host immune cells. Because host T cells in blood are depleted by conditioning regimens, it is
83 assumed that host T cell immunity is abrogated. Therefore, the role of tissue dwelling host T cells in human GVHD has
84 not been investigated.

85 T cells were once thought to populate exclusively blood and secondary lymphoid organs at steady state. However,
86 more recent observations suggest that the majority of memory T cells actually reside in human peripheral tissues,
87 primarily in those in contact with the external environment: skin, gut, liver and lung (9-13). Interestingly, these are the
88 four tissues primarily affected by GVHD in human HSCT recipients. This novel population of tissue-resident T cells has
89 been recognized to play key roles in human health and disease (reviewed in (14-16)). Clinical observations suggest that
90 skin-resident T cells survive “lymphocyte-depleting” chemotherapy, as patients who are profoundly lymphopenic
91 following chemotherapy can still develop T cell-mediated drug rashes despite the absence of circulating lymphocytes.
92 Skin biopsies from these patients demonstrate ample T cell infiltrates expressing markers consistent with tissue-resident
93 memory T cells (Divito, S.J., unpublished observations and (17)). Given the apparent durability of tissue-resident T cells,
94 we hypothesized that host tissue-resident T cells survive HSCT conditioning and play a previously unappreciated role in
95 GVHD.

98 **Results**

99 *Skin host T cells survive HSCT*

100 We collected skin and peripheral blood from three male patients receiving female donor HSC grafts to determine the
101 origin of skin T cells post-HSCT. Tissues were collected on the day of admission prior to the start of conditioning and
102 again 30±6 days post-HSCT. Residual donor infusion product was also collected. Patients were conditioned with
103 fludarabine (flu) + busulfan (bu); two received myeloablative dosing and one received non-myeloablative dosing
104 (Supplemental Table 1). FFPE skin sections from post-HSCT samples were concurrently labeled via FISH for the X and
105 Y chromosomes and immunofluorescence (IF) for the T cell marker CD3 (Figure 1A). At 30±6 days post-HSCT, the
106 majority of skin T cells in all three patients were host-derived (Figure 1B) and appeared viable morphologically (Figure
107 1A). In contrast, host T cells composed the minority in peripheral blood post-HSCT by short tandem repeat (STR)
108 analysis (Figure 1B).

109 To confirm whether T cells in skin post-HSCT were host- or donor-derived, we performed high-throughput
110 sequencing of the *TCRB* gene to identify clonal populations of memory T cells (18). Unique T cell clones were identified
111 by their CDR3 sequence. In all three patients, the majority of T cell clones in skin post-HSCT were identical to host skin
112 T cell clones pre-HSCT (Figure 1C). The 20 most abundant T cell clones in host skin post-HSCT and the comparable
113 frequency of those clones in host skin pre-HSCT or donor infusion product, respectively, are shown in Figure 1D.
114 Correlation between frequency of T cell clones in host skin pre-HSCT and skin post-HSCT was high (r^2 patient 1-0.6464,
115 patient 2-0.8740, patient 3-0.5867) (Supplemental Figure 1A). In contrast, higher frequency of clones in donor cells did
116 not correlate with increased frequency in skin post-HSCT (r^2 patient 1-0.0041, patient 2-0.0142, patient 3-0.0012)
117 (Supplemental Figure 1A,B). Of the top 100 most frequent clones in host skin post-HSCT in each patient, only zero, 1,
118 and 16, respectively, were donor-derived (Supplemental Figure 1A). Thus, T cell clonality data paralleled the results from
119 FISH-IF and STR analysis.

120

121 *Host T cells are present in skin during acute GVHD*

122 Given that skin T cells survived HSCT through 30 ± 6 days, a peak time point for onset of acute GVHD (19), and that the
123 main tissues affected by GVHD are the same tissues containing large populations of tissue-resident T cells, we
124 hypothesized that host T cells would be present in skin and gut during acute GVHD. Supplemental Table 2 details
125 retrospective patient clinical data. Chemoimmunotherapeutics received by each patient prior to transplant are detailed in
126 Supplemental Tables 3,4. Skin biopsies from 26 male patients with acute GVHD who received female donor transplants
127 were labeled via FISH-IF to determine the number and percentage of host and donor T cells (Figure 2A,B). Host T cells
128 were observed in skin during acute GVHD of all patients studied, regardless of the conditioning regimen (myeloablative,
129 median 39%, range 4-100%) (non-myeloablative, median 58%, range 3-78%) ($P=0.24$, Mann-Whitney, two-tailed)
130 (Figure 2B). Host T cells were observed throughout the skin, including within the epidermis and at the dermal-epidermal
131 junction, the primary sites of damage in acute skin GVHD (Supplemental Figure 2).

132 We anticipated that the percent host T cells might decline with time post-HSCT, as host T cells die off and/or as
133 donor T cells accumulate in skin. We did not detect a statistically significant decrease in the percent of host T cells in
134 either the myeloablative or non-myeloablative groups by linear regression (slope -0.1384 , $P=0.09$; slope 0.01133 , $P=0.94$,
135 respectively), though there were a limited number of patients at late time points (Supplemental Figure 3A). There was no
136 effect of patient age, GVHD prophylactic regimen, or type of donor transplant on percent host T cells in skin
137 (Supplemental Figure 3B,C,D).

138 To validate our FISH-IF results using a different approach, we used STR analysis on DNA from T cells extracted
139 from an acute GVHD skin specimen (FFPE) via laser capture microscopy. STR analytic data are shown for the most
140 recently obtained patient skin specimen, as DNA is highly degraded in older FFPE samples and approximately 100
141 microns of tissue was necessary to perform the assay. In this sample, STR analysis demonstrated 25% host T cell
142 chimerism in skin; this is compared to the 20% host T cells enumerated via FISH-IF in the same specimen (Supplemental
143 Figure 4). This provides independent validation of the use of FISH-IF to quantify T cell chimerism.

144 To determine whether host T cells in skin included both CD4 and CD8 T cell subsets, representative patient skin
145 sections were labeled via FISH-IF for CD3 and CD4. Multi-spectral microscopy/imaging software revealed the presence
146 of both host $CD4^+CD3^+$ T cells and presumptive $CD4^-(CD8^+)CD3^+$ T cells in skin specimens (Figure 2C). Though $CD4^+$

147 CD3⁺ cells could theoretically be $\gamma\delta$ T cell type and negative for both CD4 and CD8, Norton et al., previously reported
148 that $\gamma\delta$ T cells constitute a small fraction (~4%) of T cells in skin during acute GVHD (20). We confirmed in a subset of
149 our patients (n=5) that the majority of T cells in skin during acute GVHD were $\alpha\beta$ type not $\gamma\delta$ type T cells (Supplemental
150 Figure 5). Thus, our data demonstrate the presence of both CD4 and CD8 $\alpha\beta$ TCR host T cells in acute GVHD skin
151 lesions.

152 Given the discordance in T cell chimerism between skin and blood observed in our patients post-HSCT, we
153 compared T cell chimerism in skin and blood for patients diagnosed with acute GVHD. Seventeen of the 26 patients in the
154 retrospective acute GVHD skin cohort had PBMCs collected at/near the time of acute skin GVHD. T cells were positively
155 selected from PBMCs, purity was confirmed via flow cytometry (not shown), and T cell DNA was extracted and analyzed
156 via STR analysis. Results demonstrated a clear population of residual host T cells in skin (determined via FISH-IF)
157 despite the near or complete absence of host T cells in blood (determined by STR analysis) from paired specimens
158 (P<0.001, Wilcoxon signed rank test, two-tailed) (Figure 2D). This lack of concordance between skin and blood supports
159 the findings from our prospective cohort study.

160

161 *Host T cells are present in gut during acute GVHD*

162 To assess host T cells in gut, a retrospective cohort study (Supplemental Table 2) of 15 male patients transplanted with
163 female donor grafts who were diagnosed clinically and histopathologically with acute colonic GVHD were studied. In this
164 study, FISH-IF for both CD3 and CD8 revealed host CD8⁺CD3⁺ T cells and CD8⁻ (CD4⁺) CD3⁺ T cells in the gut of all
165 patients studied (Figure 3A,B). Host T cells were present regardless of whether patients received myeloablative or non-
166 myeloablative conditioning (myeloablative, median 22%, range 6-87%) (non-myeloablative, median 12%, range 7-41%)
167 (P=0.27, Mann-Whitney, two-tailed) (Figure 3B) and were present within both colon lamina propria and epithelium
168 (Supplemental Figure 6A,B). There were no significant differences in CD8⁺ or CD4⁺ T cell subsets between conditioning
169 regimens (Supplemental Figure 6C).

170 The percent host T cells in acute gut GVHD specimens did not show a statistically significant decrease with time
171 combining myeloablative and non-myeloablative groups (linear regression, slope -0.10, P=0.54), though again there were
172 limited number of patients at later time points (Supplemental Figure 7A). As was the case in skin, host T cell chimerism in
173 gut significantly diverged from peripheral blood (Wilcoxon signed rank test, two-tailed, P=0.01) (Figure 3C). There was
174 no association observed between the percent host T cells and age at time of transplant or type of donor transplant
175 (Supplemental Figure 7B,C).

177 *Host T cell chimerism in skin is impacted by acute GVHD*

178 To further elucidate the impact of time and acute GVHD on host T cell chimerism in peripheral tissue, skin was
179 sampled in an additional prospective patient cohort (referred to as UK cohort). Supplemental Table 5 details UK cohort
180 clinical data which was originally described in (21). In this prospective cohort, skin samples were collected for T cell
181 analysis from 34 patients at 40, 100, and/or 365 days post-transplant (8 patients were biopsied at two time points and 3
182 patients were biopsied at all three time points). Samples were categorized by whether each patient had no acute skin
183 GVHD, active acute skin GVHD, or history of acute skin GVHD that was resolved at time of biopsy. Active acute skin
184 GVHD was further divided into new onset acute skin GVHD at time of biopsy or acute skin GVHD at time of biopsy plus
185 prior episode of acute skin GVHD (Figure 4A,B). Chimerism was quantified by sequential FISH-IF performed on
186 cytopspins of migratory cells (Figure 4C). Similar to above observations, data from this cohort demonstrate that in the
187 absence of acute skin GVHD, host T cells comprised the majority of T cells in skin through one-year post-transplant (40
188 days, n=6, median 97%, range 69-100%; 100 days, n=12, median 69%, range 7-100%; 365 days, n = 1, 56%) (Figure
189 4A,B). Though there was a small decrease in median percentage host T cells with time, this was not statistically
190 significant (P>0.05, Dunn's multiple comparison's test, 40 vs 100 days). Moreover, skin samples from new onset active
191 acute GVHD likewise contained substantial host T cell populations (40 days, n=4, median 79%, range 39-93%; 100 days,
192 n = 1, 28%) (Figure 4A,B). This parallels findings from the above retrospective cohorts and supports that the proportion
193 of host versus donor T cells may not be a critical factor in the development of acute GVHD.

194 Interestingly, dividing active acute GVHD into new onset acute disease vs active disease in a patient with history
195 of acute skin GVHD revealed that a prior history of acute skin GVHD was overall associated with reduced host T cell
196 chimerism in skin (Figure 4A,B). In keeping with this observation, median host T cell chimerism was also low in skin of
197 patients who previously had acute GVHD (i.e. biopsy taken after GVHD resolution). This finding was not universal
198 though, as some patients retained substantial percentages of host T cells despite history of acute GVHD (Figure 4A,B).
199 This data suggest that acute GVHD (or its treatment) may preferentially eliminate host T cells from skin, but that in some
200 cases stable mixed chimerism can occur.

202 *Host T cells are activated in acute GVHD*

203 One patient from the retrospective cohort demonstrated 100% host T cells in skin (i.e., donor T cells could not be
204 identified), and another patient 95% host T cells in skin, during acute GVHD. Both patients had stage 1 skin disease. An
205 additional patient demonstrated 100% host T cells in skin during acute GVHD; however, he was excluded from the study
206 because there was insufficient biopsy material available for further analysis (not shown). The cohort patient with 100%
207 host T cells received anti-thymocyte globulin (ATG) as part of his conditioning regimen. ATG would be expected to
208 deplete all circulating (donor plus host) T cells (22), but it appears that non-circulating tissue-resident host T cells were
209 spared. There is precedent that depleting antibody therapies deplete circulating but not skin-resident T cells (23).

210 Figure 5A illustrates the degree of tissue damage observed in the patient with 100% host T cells in skin during
211 acute GVHD. Immunofluorescent staining demonstrated that a subset of host CD3⁺ T cells in skin in this patient were in
212 cell cycle (Ki67⁺) (Figure 5B) and that a subset of CD3⁺ T cells expressed the pro-inflammatory cytokines IFN γ and IL-17
213 in situ (Figure 5C). There were no detectable Foxp3⁺ T cells (regulatory T cell marker) or IL-10 (an immuno-regulatory
214 cytokine) producing T cells observed in this patient's skin (not shown).

215 We could not reliably perform IF staining for cytokines in conjunction with FISH labeling due to technical
216 limitations. However, because Ki67 is expressed only in activated T cells that have entered the cell cycle, FISH-IF for
217 Ki67 and CD3 was performed in gut GVHD samples as a surrogate for activation. Importantly, a lack of Ki67 does not
218 mean that a T cell is not activated, as activated memory T cells may remain in G₀ (24). Ki67 was expressed by host CD3⁺

219 T cells in colon specimens in 12 of 15 patients with a median of 5% (range 0-30%) (Figure 5D). Cumulatively, these data
220 suggest that at least a subset of host T cells are activated and contributing to the inflammatory milieu during acute GVHD.

221 Lastly, there was no statistically significant association between the percent host or donor T cells and clinical or
222 histological disease severity in skin (Kruskal-Wallis, P=0.39 and P=0.51, respectively) or in gut (Kruskal-Wallis, P=0.34
223 and P=0.38, respectively) (Figure 5E) suggesting that the proportion of host and donor T cells in skin or gut per se is not a
224 key determinant for acute GVHD severity.

225 226 *Donor APC infiltrate peripheral tissue in high numbers during acute GVHD*

227 This data raise the question of how host T cells could become activated in peripheral tissues post-HSCT. The
228 accompanying paper by Jardine *et al.*, demonstrates that donor monocyte-derived macrophages infiltrate skin during acute
229 GVHD in high numbers, and at least ex vivo, are capable of presenting antigen to and stimulating allogeneic T cells. In
230 concordance, we observed by FISH-IF that the majority of HLA-DR⁺ (class II⁺) CD3⁻ APC were of donor origin (Y
231 negative) (median 92%, range 76-100%) (P=0.004 compared to T cells, Wilcoxon signed rank test, two-tailed) in the gut
232 during acute GVHD and could be found adjacent to host (Y positive) CD3⁺ T cells (Supplemental Figure 8A,B).

233 234 *Donor monocytes with host skin resident T cells induce a GVHD-like dermatitis in the absence of donor T cells*

235 Based on these findings, we used a human engrafted mouse model to test the ability of host skin T cells to mediate GVHD
236 in the absence of donor T cells. NSG mice were grafted with healthy adult human skin, which contains abundant memory
237 T cells (“host”). These grafted mice were then subsequently adoptively transferred with “donor” (i) allogeneic CD25-
238 depleted PBMC (to deplete donor regulatory T cells), (ii) allogeneic positively selected monocytes, or (iii) saline (Figure
239 6A). Adoptively transferred PBMC contained donor T cells, whereas mice injected with monocytes were devoid of donor
240 T cells. Adult human skin has been estimated to contain roughly 1 million memory T cells/cm², the majority of which are
241 non-recirculating resident memory T cells (12, 25). Therefore, the only T cells in monocyte-infused mice were those

242 derived from the “host” adult skin graft. Grafts were harvested three weeks after donor cell infusion and analyzed by
243 histology, quantitative RT-PCR and high throughput TCR sequencing (HTS).

244 A GVHD-like dermatitis developed in skin grafts; this was characterized by acanthosis, parakeratosis, basal layer
245 vacuolization, keratinocyte dyskeratosis, lymphocyte exocytosis into the epidermis and dermal lymphocytic infiltration
246 (Figure 6B-D). Remarkably, histopathological findings were similar between skin grafts in mice injected with PBMC vs.
247 monocytes alone. Severity, as determined via histologic grading, was mildly but not significantly reduced in the absence
248 of infused donor T cells (monocyte-infused group) (Figure 6E).

249 T cell numbers in the skin grafts of monocyte- and PBMC-injected mice were not significantly different, as
250 assessed by quantitative RT-PCR for *CD3E* gene expression (Figure 6F) and HTS of the *TCRB* gene (Figure 6G). *TNFA*,
251 *IL-9*, *IL-17A* and *IL-22* levels in the skin graft, assessed by quantitative RT-PCR, were also similar in monocyte- and
252 PBMC-injected mice (Supplemental Figure 9A-D). *IFNG* was the only cytokine significantly increased in PBMC versus
253 monocyte-injected mice (Supplemental Figure 9E).

254 We next studied skin grafts by HTS of the *TCRB* gene to determine if host skin-resident T cell clones proliferated
255 and expanded in situ in the skin after encounter with donor monocytes. We identified skin-resident T cell clones by CDR3
256 sequences that were present in both saline-injected and monocyte-injected mice grafted with skin from the same donor.
257 We measured the frequency of these common clones in saline- vs. monocyte-injected mice to determine cell proliferation.
258 The frequency of host skin-resident T cell clones was increased in the skin grafts of monocyte-injected mice, suggesting
259 local proliferation and expansion within the skin (Figure 6H). Parallel analyses of PBMC-injected mice also showed host
260 skin T cell expansion, but this was not significantly different between monocyte-injected and PBMC-injected mice
261 (Figure 6I).

262 To confirm that host skin T cells were responsible for the GVHD-like dermatitis observed in monocyte-injected
263 mice, we grafted mice with human foreskin, a tissue that contains APC but few if any resident memory T cells (24).
264 Foreskin-grafted mice were injected iv with allogeneic monocytes alone or with CD25-depleted PBMC. Mice injected
265 with PBMC developed a robust GVHD-like dermatitis. In contrast, monocyte-injected mice bearing skin grafts that lacked

266 host T cells did not develop inflammation (Figure 6J), indicating that the dermatitis observed in adult skin grafted mice
267 was mediated by host skin-resident T cells.

268

269 Discussion

270 It has long been presumed that T cell chimerism in blood and bone marrow reflects T cell chimerism in all peripheral
271 tissues, based on the assumption that conditioning regimens deplete host T cells in blood, bone marrow, and peripheral
272 tissues equally. The appreciation that memory T cells are abundant in human peripheral tissues, however, is relatively
273 recent (reviewed in (11, 14-16)). In our studies, host T cell chimerism in skin and gut diverged markedly from host T cell
274 chimerism in blood, indicating that T cells resident in peripheral tissues are highly resistant to depletion, even after high-
275 intensity conditioning. Therefore, an important finding of this study is that T cell chimerism in blood and/or bone marrow
276 does not reflect, and should not be used to assess, chimerism in peripheral tissues. This is notable because T cells are
277 more abundant in peripheral tissues than in circulation (25).

278 Given that skin-resident T cells appear to survive HSCT conditioning and that the tissues known to contain large
279 numbers of resident T cells are the main target organs in GVHD, we hypothesized that host T cells would be present in
280 target tissues during acute GVHD. Using two retrospective cohorts totaling 41 patients across two countries, and a
281 prospective cohort of 34 patients from a third country, we observed host T cells in skin and colon during acute GVHD.
282 While this study could not determine with certainty the origin of the host T cells (tissue-resident vs migratory), the
283 efficacy of conditioning regimens at depleting circulating T cells strongly suggests that the surviving host T cells were
284 predominantly resident in tissue in situ. A prospective study tracking T cell clones pre-HSCT through the post-HSCT
285 period and during acute GVHD will be necessary to address this.

286 Our data support previous findings that T cells in peripheral tissues during acute GVHD bear $\alpha\beta$ TCRs rather than
287 $\gamma\delta$ TCRs (20, 26). Attempts at staining for NKT cells or mucosal associated invariant T cells (which could be
288 phenotypically CD3⁺CD4⁻CD8⁻) using antibodies for V α 24-J α 18 and V α 7.2, respectively, were unsuccessful in our FFPE
289 samples. Thorough analysis of these populations would require flow cytometry performed on freshly collected tissue,
290 though would be interesting given findings that suggest invariant NKT cells may play a regulatory role in GVHD (27).

291 Korngold and Sprent showed 40 years ago that donor T cells responding to host allo-antigen are required for
292 GVHD in a mouse model (28). Nearly all subsequent mouse models of GVHD have been engineered under the
293 assumption that donor T cells are both necessary and sufficient for acute GVHD. In review of the literature, two GVHD

294 mouse studies, utilizing naïve donor to naïve recipient, investigated host T cells in lymphoid tissues that survived
295 conditioning. These data suggested a possible regulatory role for host T cells against chronic GVHD (29) and donor
296 lymphocyte infusion-associated GVHD (30). Our data support a pro-inflammatory role for host T cells in peripheral
297 tissues, though our study focused on acute rather than chronic GVHD, and only one patient had received donor
298 lymphocyte infusion. Notably, GVHD mouse models nearly always employ naïve donor and recipient mice housed in
299 specific pathogen free conditions. Importantly, these mice typically lack the robust and diverse memory T cell population,
300 in particular tissue-resident memory T cells, that are present in humans (31) and that may be key contributors to skin and
301 gut GVHD.

302 The observation that a subset of host T cells in peripheral tissues were proliferating indicates that they were
303 activated and not quiescent. This is consistent with the observations from the human engrafted mouse experiments, where
304 host T cells were shown to have expanded through proliferation by molecular assessment of *CD3E* mRNA and *TCRB*
305 DNA. Host T cells could clearly mediate a GVHD-like process in our human-engrafted mouse model, as host skin T cells
306 and positively selected donor monocytes were sufficient to induce a GVHD-like dermatitis. Histopathologic severity in
307 the donor monocyte only injected mice was slightly but not significantly reduced compared to mice that received donor T
308 cells (CD25-depleted PBMC-injected mice). Grafts with skin-resident T cells from mice injected with donor monocytes
309 but not donor T cells contained *IL-17*, *IL-22* and *TNFA* comparable to mice receiving donor T cells suggesting that
310 production of these cytokines was due to host skin-resident T cells. The addition of donor T cells to the humanized mouse
311 model resulted in significantly increased *IFNG* within grafts suggesting that Th1 polarization may be responsible for the
312 increased disease severity observed in mice receiving donor T cells.

313 The observation that one patient manifested 100% host T cell chimerism and another patient 95% host T cell
314 chimerism in skin during acute GVHD supports the idea that host T cells may be sufficient for what was clinically and
315 histopathologically diagnosed as GVHD, and that the (near complete) absence of donor T cells may result in a milder
316 form of GVHD. Interestingly, depletion of CD45RA⁺ naïve T cells from allogeneic grafts prior to transplantation does not
317 reduce the incidence of acute GVHD but does reduce disease severity (32), supporting our observations. It is seemingly
318 plausible that while both donor and host T cells may be required for severe acute GVHD, host T cells alone may be

319 sufficient for less florid GVHD. Whether host T cell activation synergizes with donor T cell activation to generate a more
320 severe phenotype cannot be determined from these experiments.

321 This prompts the question of whether donor and host T cells can coexist. Intriguingly, it may be the attempt of
322 host and donor T cells to eliminate each other that is part and parcel with GVHD. To this point, Figure 4A shows that the
323 percentage of host T cells in skin is reduced in patients with prior/resolved GVHD, suggesting that acute GVHD (or its
324 treatment) may preferentially eliminate host T cells from skin. However, there were multiple cases in this same cohort
325 where substantial host T cell populations remained despite prior/resolved acute GVHD supporting that stable mixed
326 chimerism is possible in peripheral tissues despite GVHD. Stable mixed chimerism in circulating T cell populations post-
327 stem cell transplantation has been previously reported by multiple groups indicating the possibility of mutual “tolerance”
328 (33-36). The same appears to be true in peripheral tissues as well in the setting of solid organ transplantation (37, 38).

329 Residual host T cells in circulation/lymphoid organs is a risk factor for graft rejection (39-41), though residual
330 host T cells in peripheral tissues in relation to graft rejection has not been studied. None of the patients in our cohorts had
331 graft rejection. Given the marked divergence in T cell chimerism between peripheral tissues (skin/gut) and blood observed
332 in this study, we would hypothesize that graft rejection would more likely align with residual T cell populations in
333 circulation and bone marrow/lymphoid organs rather than host T cell populations in peripheral tissues. However, we
334 cannot draw any definitive conclusions from our data, and this is an area of investigation to be pursued.

335 The effect of T cell depletion on GVHD is an important issue as it is commonly presumed that T cell depletion
336 abrogates GVHD and therefore donor T cells are necessary, and host T cells insufficient, for disease. However, even with
337 complete T cell depletion from donor grafts, the reduction in acute GVHD incidence is highly variable across studies and
338 is not absolute (reviewed in (42)). Whether the variable results are due to incomplete donor T cell depletion or to residual
339 host T cells is unclear. Further, studies often report a reduction in grade II-IV disease but do not comment on incidence of
340 mild GVHD, where host T cells may be prominently involved. Most importantly, commonly used T cell depletion
341 strategies have significant off-target effects. For example, alemtuzumab may deplete and/or reduce functionality of
342 monocytes and monocyte-derived APC in addition to T cells (43, 44). Based on our data, donor monocytes may be critical
343 in stimulating host T cell mediated-GVHD. ATG likewise targets numerous cell populations including APC (45). Even in
344 a study using anti-CD2 and anti-CD3 antibodies which would be expected to target only T cells (and potentially NKT

345 cells), an effect on the myeloid compartment was reported by investigators (46). Further studies are clearly needed to
346 delineate a potential role for host T cells in GVHD in T cell depleted grafts.

347 These data also raise the question of GVHD incidence and severity in patients transplanted for severe combined
348 immunodeficiency (SCID), a rare genetic disease affecting T (and potentially B and NK) cell development or function
349 (47). SCID patients can develop GVHD (47-51). Though this might suggest that donor T cells alone are sufficient for
350 GVHD, several factors complicate interpretation of this observation. First, GVHD data are quite sparse in SCID patients
351 due to the rarity of disease and to the variability in conditioning, donor stem cell source, and GVHD prophylaxis used in
352 each patient (47-49, 51). Moreover, the SCID phenotype is quite heterogeneous as it is caused by mutations in several
353 different genes; in fact some SCID patients have circulating T cells (47). The question of whether these patients also have
354 tissue-resident T cells has not been addressed to our knowledge. Interestingly, there are reports of SCID patients receiving
355 T cell depleted donor stem cells yet developing GVHD (49, 51). Whether these patients had functional host T cells in
356 tissue or developed GVHD from incomplete donor T cell depletion is unclear. Deeper interrogation of GVHD in SCID
357 patients may yield valuable insight into the relative contributions of donor and host T cells to disease.

358 There are several potential mechanisms by which host T cells might become activated even in a fully MHC-
359 matched allogeneic transplant. Donor or host APC expressing self-MHC could present minor-mismatched alloantigen to T
360 cells. Host APC could present neo-antigens expressed in the setting of conditioning-induced tissue damage which would
361 be viewed by T cells as foreign, or self-peptides with loss of T cell tolerance in the setting of robust inflammation. Lastly,
362 antigen-independent bystander activation of T cells via cytokine stimulation could occur. Haniffa et al., evaluated
363 chimerism of different skin APC populations following HSCT. Dermal dendritic cells had high turnover, Langerhans cells
364 intermediate turnover, while host resident macrophages persisted long-term in skin post-transplant in the absence of
365 GVHD (21). The accompanying paper by Jardine et al., illuminates that the predominant APC population present in skin
366 during active acute GVHD is donor CD11c⁺CD14⁺ monocyte-derived macrophages, and that these APC are capable of
367 activating allogeneic T cells ex vivo. We similarly observed donor APC infiltrating gut in high percentages during acute
368 GVHD, supporting the possibility of donor APC: host T cell interaction. The human-engrafted mouse model demonstrated
369 that the combined presence of host skin T cells and donor monocytes induced GVHD-like dermatitis, but the absence of
370 either cell population prevented disease. Whatever the mechanism, our observations suggest the term “Graft Versus Host

371 Disease” does not fully describe the pathophysiology, as “host vs graft” events appear to contribute to the clinical and
372 histopathological appearance of this disease. Importantly, this data does not in any way argue against the role of donor T
373 cells in GVHD.

374 This study reveals a novel avenue of research into the pathophysiology of GVHD. The limitations of this study
375 include the small sample sizes and the retrospective nature of the human acute GVHD studies necessitating use of FFPE
376 specimens. Archival FFPE tissue is more challenging to stain via IF (due to crosslinking of epitopes by formalin) and can
377 suffer from DNA degradation thus hampering FISH. More extensive analysis of host T cells in patient samples was
378 therefore precluded. Moving forward, a large prospective human study in which fresh tissue is collected will allow for
379 deeper interrogation of host T cell phenotype and function. Coupled with humanized mouse models, such studies will be
380 able to evaluate the true contribution of host T cells to acute GVHD. Though challenging, these studies should be pursued
381 given the possible significant implications for clinical care.

382 **Methods**

383 **Patients**

384 Prospective study (USA cohort): adult males undergoing a first allogeneic HSCT receiving female donor grafts were
385 enrolled. Subjects with underlying T cell malignancies or HIV were excluded. Skin biopsy and peripheral blood were
386 collected on the day of admission for transplantation prior to conditioning and again 30±6 days post-HSCT. Additionally,
387 residual donor cells from the stem cell product bag were collected. Written informed consent was obtained from each
388 patient.

389 Prospective study (UK cohort): adult females undergoing a first allogeneic HSCT receiving male donor grafts
390 were enrolled. Skin biopsies were collected at 40, 100 and/or 365 days post-transplant. Written informed consent was
391 obtained from each patient.

392 Retrospective studies: sections were obtained from FFPE skin (Brigham and Women's Hospital/Dana Farber
393 Cancer Institute) or colonic (Oslo University Hospital) biopsies previously acquired for clinical purposes from adult male
394 patients transplanted from female donors. Because biopsies were collected for clinical purposes, they were obtained at
395 variable time points after disease onset so in some cases were collected after initiation of systemic immunosuppression.
396 Medical record review confirmed that each patient was diagnosed clinically with acute skin or gut GVHD, and each
397 patient's tissue biopsy was read by an experienced pathologist as consistent with GVHD. Samples were excluded from
398 any patient with underlying T cell malignancy or history of prior transplant, or from patients with limited available tissue
399 sample. PBMCs taken during the same episode of acute GVHD were available for analysis for some patients.

400 For simplicity, reduced-intensity and non-myeloablative conditioning regimens have been combined and are
401 referred to as "non-myeloablative" conditioning to distinguish them from myeloablative conditioning.

402

403 **T cell selection from PBMCs and Flow cytometry**

404 Skin cohort - T cells were positively selected from PBMCs using human CD3 positive selection kit (Stem Cell
405 Technologies). Percentage selection was confirmed by staining for CD2 (RPA-2.10, 300213, Biolegend) and analysis on a
406 FACSCanto flow cytometer (BD Biosciences).

407

408 **High-throughput TCR β sequencing**

409 DNA was extracted from ~80-100 microns of OCT embedded frozen skin specimens using QIAamp DNA Micro Kit or
410 from PBMCs or T cells positively selected from PBMCs using the QIAamp DNA Mini Kit, both according to
411 manufacturer's protocol (Qiagen). ImmunoSEQ high-throughput *TCRB* sequencing was performed (Adaptive
412 Biotechnologies).

414 **Immunohistochemistry**

415 FFPE skin sections (5-6 μ m) from 5 retrospective skin cohort patients were stained via immunohistochemistry for delta
416 TCR clone H-41 (Santa Cruz Biotechnologies) following EDTA antigen retrieval or betaF1 clone 8A3 (ThermoFisher
417 Scientific) following enzyme antigen retrieval with Carezyme III: Pronase Kit (Biocare Medical). Slides were developed
418 with 3,3'-diaminobenzidine tetrahydrochloride (DAB).

420 **Laser Capture Microscopy for CD3⁺ T Cells**

421 FFPE skin sections (10 μ m) from a retrospective skin cohort patient were stained via immunohistochemistry for CD3
422 (LN10, NCL-L-CD3-565, Leica Biosystems) with (DAB) following acidic antigen retrieval. CD3⁺ cells were isolated
423 using a PALM MicroBeam laser capture microscope with PALM RoboSoftware (ZEISS). DNA was extracted from the
424 collected material using QIAamp DNA FFPE Tissue Kit according to manufacturer's instructions (Qiagen).

426 **Short Tandem Repeat (STR) Analysis**

427 Skin cohort - DNA from T cells isolated from skin and peripheral blood were analyzed via STR analysis using Promega's
428 Powerplex 21 system (Promega Corporation) with subsequent run on an ABI 3130 Genetic Analyzer (Thermo Fisher
429 Scientific Inc.).

430 Colon cohort - Chimerism was performed by the department of forensic medicine, Oslo University Hospital, as part of
431 routine analysis following HSCT. PCR amplification and STR analysis was performed using Promega PowerPlex fusion
432 6C system (Promega Corporation).

433

434 **Immunofluorescence (IF)**

435 FFPE skin sections 5-6 μm thick were baked, deparaffinized, and rehydrated. Skin sections underwent acidic antigen
436 retrieval at 96°C, were blocked for non-specific protein binding, then stained for mouse anti-human CD3 with either anti-
437 human Ki67 (SP6, ab16667, Abcam), IL-17 (polyclonal, LS-C104427, LifeSpan Biosciences) or IFN γ (polyclonal,
438 ab25101, Abcam), followed by secondary staining with different combinations of anti-rabbit (Poly4064, 406412,
439 Biologend), mouse (Poly4053, 405324, Biologend) or goat (A21432, Invitrogen/ThermoFisher) IgG AF555, and/or with
440 anti-mouse IgG AF647 (A31571, Invitrogen/ThermoFisher) or Cy2 (715-225-150, Jackson ImmunoResearch) and
441 counterstained with DAPI. Tissue was imaged using a Mantra™ Quantitative Pathology Workstation and analyzed using
442 InFORM® software (PerkinElmer).

444 **Fluorescence in situ hybridization-Immunofluorescence (FISH-IF) on FFPE tissue**

445 FFPE skin and colon sections 5-6 μm thick were baked, deparaffinized, and rehydrated. Skin sections underwent acidic
446 antigen retrieval at 96°C and pepsin treatment; colon sections underwent basic antigen retrieval at 100°C. FISH probes for
447 X and Y chromosomes (Abbott Molecular) were hybridized overnight at 37°C. Skin sections required denaturation at
448 94°C prior to hybridization. After post-hybridization washing, skin sections were blocked for non-specific protein binding
449 then stained for mouse anti-human CD3 with or without rabbit anti-human CD4 (EP204, AC-0173A, Epitomics), then
450 with anti-mouse IgG AF647 (A31571) with or without anti-rabbit IgG AF594 (A11012, Invitrogen/ThermoFisher) and
451 counterstained with DAPI. Tissue was imaged using a Mantra™ Quantitative Pathology Workstation and analyzed using
452 InFORM® software (PerkinElmer). Colon sections were stained with rabbit anti-human CD3 (polyclonal, A045201,
453 DAKO/Agilent), mouse anti-human CD8 (4B11, NCL-L-CD8-4B11, Novocastra), mouse anti-human HLA-DR
454 (TAL.1B5, M074601, DAKO), and/or mouse anti-human Ki67 (MIB-1, sc-101861, Santa Cruz Biotechnology) and
455 secondary antibodies for anti-rabbit IgG AF647 (A31573) and AF555 (A31572), anti-mouse IgG2b AF555 (A21147),
456 anti-mouse IgG1 AF647 (A21240) and/or anti-mouse IgG1 AF555 (A21127) (all Invitrogen/ThermoFisher). After
457 counterstaining with Hoechst, sections were mounted with Prolong Diamond. Slides were inspected by confocal
458 microscopy, Olympus FV1000 (Olympus) and analyzed digitally using ImageJ.

459

460 **FISH-IF on cytopins of dermal T cells**

461 Dermal T cells were isolated from shave skin biopsies by migration as described in (21) Briefly, epidermal and dermal
462 sheets were separated by digestion in 1 mg/ml dispase (Invitrogen) in RPMI (Invitrogen) for 60 min at 37°C. Dermal
463 sheets were cultured in X-Vivo 10 (Cambrex) with 500 U/ml GM-CSF (Sargramostim; Durbin PLC) and migrating cells
464 harvested onto cytopin slides after 60-82 hours. Cytopin slides were air dried and stored at -20°C before sequential
465 immunofluorescence and FISH. Slides were thawed and fixed in methanol then stained with antibodies to CD3 (SK7,
466 347340, BD), and Alexa Fluor 633–conjugated goat anti–mouse IgG1 (A-21126, Thermofisher). Myeloid cells were
467 identified with antibodies to HLA-DR-FITC (L243, 347363, BD), CD14 (rabbit polyclonal, 106285, Abcam) and FXIIIA
468 (sheep polyclonal, SAF13A-AP, Enzyme Research Laboratories) as previously described (21). Ten to twelve four-color
469 images were acquired by confocal microscopy and assembled into montages using Photoshop CS2 (Adobe). Cytopin
470 slides were then fixed with methanol/acetic acid 3:1 for 5 min, probed with CEP X/Y DNA probes (Vysis, Abbott
471 Molecular), mounted with Vectastain containing DAPI (Vector Laboratories), and scored for X/Y hybridization.

472

473 **Histologic grading of human skin and colon**

474 For skin, a modified Lerner system (52) was used based on findings by Darmstadt et al. (53) whereby Grade 2 was
475 subdivided into 2a and 2b based on ≤ 4 dyskeratotic epidermal cells per linear mm epidermis or > 5 dyskeratotic
476 epidermal cells per linear mm epidermis, respectively. For gut, a modified Lerner system (52) was used based on findings
477 by Lin et al. including patients with 2-5 crypt apoptotic bodies per 10 contiguous crypts that had typical clinical signs of
478 GVHD, as histologic Grade 1 (54).

479

480 **Human engrafted mouse studies: Human skin and blood samples**

481 Blood from healthy individuals was obtained after leukapheresis. Skin from healthy adult patients was obtained from
482 patients undergoing cosmetic surgery procedures and neonatal foreskin was obtained from infants circumcised at Brigham
483 and Women’s Hospital.

484

485 **Isolation of CD25-depleted PBMC and monocytes from human peripheral blood**

486 Magnetic-activated cell sorting (MACS) was used to prepare CD25-depleted PBMC and purified monocytes for injection.
487 CD25-depleted PBMC were prepared by negative selection and CD14⁺ monocytes were prepared by positive selection.
488 Briefly, cells were resuspended in cold separation buffer (phosphate-buffered saline (PBS) containing 0.5% bovine serum
489 albumin (BSA) and 2 mM EDTA; both from Sigma-Aldrich), incubated for 15 min at 4°C with anti-CD25 or anti-CD14
490 Microbeads (Miltenyi Biotec), washed by adding 5 ml of separation buffer and centrifuged at 300 × g for 10 min. Cells
491 were resuspended in 500 µl of separation buffer and applied onto an autoMACS Pro (Miltenyi Biotec) instrument for
492 magnetic separation. The negative eluted fraction was used for CD25-depleted PBMC and the positive eluted fraction was
493 used for monocyte separations.

494

495 **Human engrafted mouse model**

496 Adult human skin thinned with an electric dermatome or full thickness neonatal foreskin was grafted onto the backs of 6-
497 to 8-week old female and male nonobese diabetic/severe combined immunodeficient/IL-2 receptor γ chain^{null} mice (NSG,
498 Jackson Laboratory). Three weeks later, i) saline solution, ii) 5 × 10⁶ allogeneic CD25-depleted PBMCs or iii) 5 × 10⁶
499 allogeneic monocytes were injected into mice via retro-orbital injection. The skin grafts were harvested for analysis three
500 weeks after injection of cells.

501

502 **Immunohistochemical studies**

503 H&E stains were carried out on FFPE tissue sections (4 µm) by standard immunohistochemical techniques.

504

505 **RNA isolation and quantitative real-time PCR**

506 Total RNA was extracted from skin grafts using the RNeasy Lipid Tissue kit (Qiagen). The concentration and purity of
507 the isolated RNA was determined using a NanoDrop instrument (Thermo Scientific). Total RNA was reverse transcribed
508 to cDNA using the SuperScript VILO cDNA Synthesis Kit (Life Technologies). Quantitative real-time PCR was
509 performed using the ABI StepONE Plus instrument and the Fast SYBR Green Master Mix (Applied Biosystems).

510 Expression of each gene transcript was determined relative to the housekeeping gene transcript, *B-Actin*, and calculated as
511 $2^{-(C_t \text{ Transcript} - C_t \beta\text{-Actin})}$. Primer pairs were purchased from Integrated DNA Technologies. The primer sequences

512 were: *CD3E*: Forward: GGGGCAAGATGGTAATGAAG; Reverse: CCAGGATACTGAGGGCATGT. *IL-9*: Forward:
513 TCTGGTGCAGTTGTCAGAGGGAAT; Reverse: TGCAGGAAGATCCAGCTTCCAAGT. *IL-17A*: Forward:
514 CCACGAAATCCAGGATGCCCAAAT; Reverse: ATTCCAAGGTGAGGTGGATCGGTT. *IL-22*: Forward:
515 AAGGTGCGGTTGGTGATATAG; Reverse: CACCAGTTGCTCGAGTTAGAA. *IFNG*: Forward:
516 CTCTTCGACCTCGAAACAGC; Reverse: TGACCAGAGCATCCAAAAGA. *TNFA*: Forward:
517 GCCAGAGGGCTGATTAGAGA; Reverse: TCAGCCTCTTCTCCTTCCTG. *B-Actin*: Forward:
518 TCACCCACACTGTGCCCATCTACGA, Reverse: CAGCGGAACCGCTCATTGCCAATGG.

520 **Statistics**

521 Clonality studies were analyzed using ImmunoSEQ ANALYZER. Remaining studies were analyzed using
522 GraphPad Prism. Comparison of two independent groups was performed using Mann-Whitney test, either one-tailed or
523 two-tailed (specified for each analysis in the results section and figure legends). Paired specimens were analyzed using a
524 two-tailed Wilcoxon signed rank test. One-way Kruskal-Wallis test was used with Dunn's post-test for comparing more
525 than two independent groups. Simple linear regression was used when both independent and dependent variables were
526 continuous. A P value < 0.05 was considered significant for all statistical tests used.

528 **Study Approval**

529 All patient studies were approved by each participating institution's ethics committee and in accordance with the
530 Declaration of Helsinki. All tissues were collected and used with prior approval from the Institutional Review Board of
531 the Partners Human Research Committee (Partners Research Management), Newcastle and North Tyneside Local
532 Research Ethics Committee 1, and the Norwegian Regional Committee for Medical Research Ethics. Animal experiments
533 were performed in accordance with the guidelines put forth by the Center for Animal Resources and Comparative
534 Medicine at Harvard Medical School, and all protocols and experimental plans were approved by the HMS IACUC
535 beforehand.

538 **Author Contributions:**

539 SJD, ATA, TM, CPE, PCH, MH, JH, GP, MC, ESB performed experimentation.

540 SJD, ATA, CPE, JTO, EM, GP, VTH, RJS, ESB, TGD, HR, JW, HTK, MCM, MC, JR, IG, CSC, RAC, FLJ, TSK
541 contributed to study design and/or analysis and interpretation of data.

542 SJD, ATA, MC, RAC, FLJ, TSK drafted the manuscript.

543

544 **Acknowledgements:**

545 The authors would like to thank the Brigham and Women's Hospital Cytogenetics core facility, Harvard Medical School
546 Neurobiology imaging unit, Zihou Yan for his assistance acquiring medical record data, and David Chiliza for his
547 assistance reviewing the manuscript. The authors would also like to thank Kjersti Thorvaldsen Hagen for her assistance
548 preparing slides for immunohistochemistry and Margrethe Rødhammer Stenersen, Norwegian Institute of Public Health,
549 who analyzed STR analysis from the retrospective gut cohort data.

550

551 **References:**

- 552 1. Tanaka Y, et al. Analysis of non-relapse mortality and causes of death over 15 years following allogeneic
553 hematopoietic stem cell transplantation. *Bone Marrow Transplant.* 2016;51(4):553-559.
- 554 2. Anasetti C, et al. Peripheral-blood stem cells versus bone marrow from unrelated donors. *N Engl J Med.*
555 2012;367(16):1487-1496.
- 556 3. Flowers ME, et al. Comparative analysis of risk factors for acute graft-versus-host disease and for chronic graft-
557 versus-host disease according to National Institutes of Health consensus criteria. *Blood.* 2011;117(11):3214-3219.
- 558 4. Inamoto Y, et al. Association of severity of organ involvement with mortality and recurrent malignancy in
559 patients with chronic graft-versus-host disease. *Haematologica.* 2014;99(10):1618-1623.
- 560 5. Pasquini MC. Impact of graft-versus-host disease on survival. *Best Pract Res Clin Haematol.* 2008;21(2):193-
561 204.
- 562 6. Jagasia M, et al. Risk factors for acute GVHD and survival after hematopoietic cell transplantation. *Blood.*
563 2012;119(1):296-307.
- 564 7. Magenau J, Runaas L, Reddy P. Advances in understanding the pathogenesis of graft-versus-host disease. *Br J*
565 *Haematol.* 2016;173(2):190-205.
- 566 8. Zeiser R, Blazar BR. Acute Graft-versus-Host Disease - Biologic Process, Prevention, and Therapy. *N Engl J*
567 *Med.* 2017;377(22):2167-2179.
- 568 9. Pallett LJ, et al. IL-2(high) tissue-resident T cells in the human liver: Sentinels for hepatotropic infection. *J Exp*
569 *Med.* 2017;214(6):1567-1580.
- 570 10. Stelma F, et al. Human intrahepatic CD69 + CD8+ T cells have a tissue resident memory T cell phenotype with
571 reduced cytolytic capacity. *Sci Rep.* 2017;7(1):6172.
- 572 11. Sathaliyawala T, et al. Distribution and compartmentalization of human circulating and tissue-resident memory T
573 cell subsets. *Immunity.* 2013;38(1):187-197.
- 574 12. Clark RA, et al. The vast majority of CLA+ T cells are resident in normal skin. *J Immunol.* 2006;176(7):4431-
575 4439.

- 576 13. Purwar R, et al. Resident memory T cells (T(RM)) are abundant in human lung: diversity, function, and antigen
577 specificity. *PLoS One*. 2011;6(1):e16245.
- 578 14. Park CO, Kupper TS. The emerging role of resident memory T cells in protective immunity and inflammatory
579 disease. *Nat Med*. 2015;21(7):688-697.
- 580 15. Schenkel JM, Masopust D. Tissue-resident memory T cells. *Immunity*. 2014;41(6):886-897.
- 581 16. Clark RA. Resident memory T cells in human health and disease. *Sci Transl Med*. 2015;7(269):269rv261.
- 582 17. Iriki H, et al. Toxic epidermal necrolysis in the absence of circulating T cells: a possible role for resident memory
583 T cells. *J Am Acad Dermatol*. 2014;71(5):e214-216.
- 584 18. Robins HS, et al. Comprehensive assessment of T-cell receptor beta-chain diversity in alphabeta T cells. *Blood*.
585 2009;114(19):4099-4107.
- 586 19. Carnevale-Schianca F, et al. Longitudinal assessment of morbidity and acute graft-versus-host disease after
587 allogeneic hematopoietic cell transplantation: retrospective analysis of a multicenter phase III study. *Biol Blood*
588 *Marrow Transplant*. 2009;15(6):749-756.
- 589 20. Norton J, al-Saffar N, Sloane JP. An immunohistological study of gamma/delta lymphocytes in human cutaneous
590 graft-versus-host disease. *Bone Marrow Transplant*. 1991;7(3):205-208.
- 591 21. Haniffa M, et al. Differential rates of replacement of human dermal dendritic cells and macrophages during
592 hematopoietic stem cell transplantation. *J Exp Med*. 2009;206(2):371-385.
- 593 22. Busca A, Aversa F. In-vivo or ex-vivo T cell depletion or both to prevent graft-versus-host disease after
594 hematopoietic stem cell transplantation. *Expert Opin Biol Ther*. 2017;17(11):1401-1415.
- 595 23. Clark RA, et al. Skin effector memory T cells do not recirculate and provide immune protection in alemtuzumab-
596 treated CTCL patients. *Sci Transl Med*. 2012;4(117):117ra117.
- 597 24. Watanabe R, et al. Human skin is protected by four functionally and phenotypically discrete populations of
598 resident and recirculating memory T cells. *Sci Transl Med*. 2015;7(279):279ra239.
- 599 25. Clark RA, et al. A novel method for the isolation of skin resident T cells from normal and diseased human skin. *J*
600 *Invest Dermatol*. 2006;126(5):1059-1070.

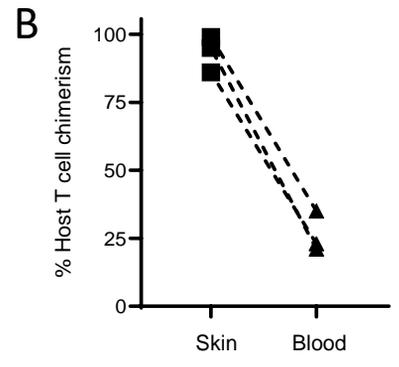
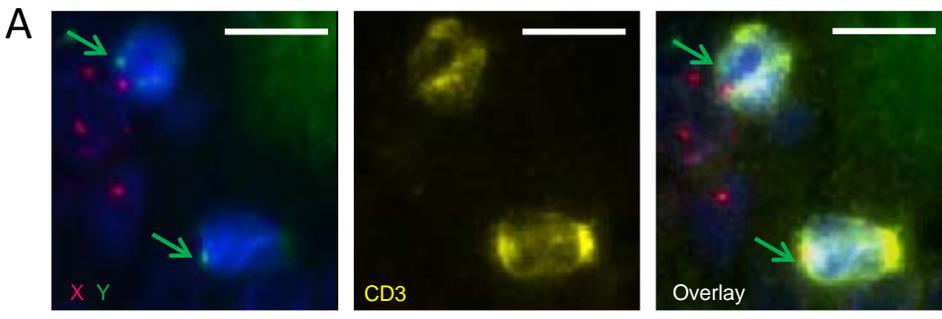
- 601 26. Norton J, al-Saffar N, Sloane JP. Immunohistological study of distribution of gamma/delta lymphocytes after
602 allogeneic bone marrow transplantation. *J Clin Pathol.* 1992;45(11):1027-1028.
- 603 27. Mavers M, Maas-Bauer K, Negrin RS. Invariant Natural Killer T Cells As Suppressors of Graft-versus-Host
604 Disease in Allogeneic Hematopoietic Stem Cell Transplantation. *Front Immunol.* 2017;8(900).
- 605 28. Korngold R, Sprent J. Lethal graft-versus-host disease after bone marrow transplantation across minor
606 histocompatibility barriers in mice. Prevention by removing mature T cells from marrow. *J Exp Med.*
607 1978;148(6):1687-1698.
- 608 29. Anderson BE, et al. Recipient CD4+ T cells that survive irradiation regulate chronic graft-versus-host disease.
609 *Blood.* 2004;104(5):1565-1573.
- 610 30. Blazar BR, et al. Host T cells resist graft-versus-host disease mediated by donor leukocyte infusions. *J Immunol.*
611 2000;165(9):4901-4909.
- 612 31. Beura LK, et al. Normalizing the environment recapitulates adult human immune traits in laboratory mice.
613 *Nature.* 2016;532(7600):512-516.
- 614 32. Bleakley M, et al. Outcomes of acute leukemia patients transplanted with naive T cell-depleted stem cell grafts. *J*
615 *Clin Invest.* 2015;125(7):2677-2689.
- 616 33. Andreani M, et al. Persistence of mixed chimerism in patients transplanted for the treatment of thalassemia.
617 *Blood.* 1996;87(8):3494-3499.
- 618 34. Andreani M, et al. Long-term survival of ex-thalassemic patients with persistent mixed chimerism after bone
619 marrow transplantation. *Bone Marrow Transplant.* 2000;25(4):401-404.
- 620 35. Sachs DH, Kawai T, Sykes M. Induction of tolerance through mixed chimerism. *Cold Spring Harb Perspect Med.*
621 2014;4(1):a015529.
- 622 36. Walters MC, et al. Stable mixed hematopoietic chimerism after bone marrow transplantation for sickle cell
623 anemia. *Biol Blood Marrow Transplant.* 2001;7(12):665-673.
- 624 37. Bartolome-Casado R, et al. Resident memory CD8 T cells persist for years in human small intestine. *J Exp Med.*
625 2019;216(10):2412-2426.

- 626 38. Snyder ME, et al. Generation and persistence of human tissue-resident memory T cells in lung transplantation. *Sci*
627 *Immunol.* 2019;4(33).
- 628 39. Nakamura H, Gress RE. Graft rejection by cytolytic T cells. Specificity of the effector mechanism in the rejection
629 of allogeneic marrow. *Transplantation.* 1990;49(2):453-458.
- 630 40. Kernan NA, Flomenberg N, Dupont B, O'Reilly RJ. Graft rejection in recipients of T-cell-depleted HLA-
631 nonidentical marrow transplants for leukemia. Identification of host-derived antidonor allocytotoxic T
632 lymphocytes. *Transplantation.* 1987;43(6):842-847.
- 633 41. Voogt PJ, et al. Rejection of bone-marrow graft by recipient-derived cytotoxic T lymphocytes against minor
634 histocompatibility antigens. *Lancet.* 1990;335(8682):131-134.
- 635 42. Ho VT, Soiffer RJ. The history and future of T-cell depletion as graft-versus-host disease prophylaxis for
636 allogeneic hematopoietic stem cell transplantation. *Blood.* 2001;98(12):3192-3204.
- 637 43. Buggins AG, et al. Peripheral blood but not tissue dendritic cells express CD52 and are depleted by treatment
638 with alemtuzumab. *Blood.* 2002;100(5):1715-1720.
- 639 44. Fabian I, et al. Effects of CAMPATH-1 antibodies on the functional activity of monocytes and
640 polymorphonuclear neutrophils. *Exp Hematol.* 1993;21(12):1522-1527.
- 641 45. Jin F, et al. Antithymocyte globulin treatment at the time of transplantation impairs donor hematopoietic stem cell
642 engraftment. *Cell Mol Immunol.* 2017;14(5):443-450.
- 643 46. Herve P, et al. Removal of marrow T cells with OKT3-OKT11 monoclonal antibodies and complement to prevent
644 acute graft-versus-host disease. A pilot study in ten patients. *Transplantation.* 1985;39(2):138-143.
- 645 47. Chinn IK, Shearer WT. Severe Combined Immunodeficiency Disorders. *Immunol Allergy Clin North Am.*
646 2015;35(4):671-694.
- 647 48. Diaz de Heredia C, et al. Unrelated cord blood transplantation for severe combined immunodeficiency and other
648 primary immunodeficiencies. *Bone Marrow Transplant.* 2008;41(7):627-633.
- 649 49. Dinardo L, Brown V, Perez E, Bunin N, Sullivan KE. A single-center study of hematopoietic stem cell
650 transplantation for primary immune deficiencies (PIDD). *Pediatr Transplant.* 2012;16(1):63-72.

- 651 50. Sato T, et al. Stem cell transplantation in primary immunodeficiency disease patients. *Pediatr Int.*
652 2007;49(6):795-800.
- 653 51. Tsuji Y, et al. Hematopoietic stem cell transplantation for 30 patients with primary immunodeficiency diseases:
654 20 years experience of a single team. *Bone Marrow Transplant.* 2006;37(5):469-477.
- 655 52. Lerner KG, et al. Histopathology of graft-vs.-host reaction (GvHR) in human recipients of marrow from HL-A-
656 matched sibling donors. *Transplant Proc.* 1974;6(4):367-371.
- 657 53. Darmstadt GL, Donnenberg AD, Vogelsang GB, Farmer ER, Horn TD. Clinical, laboratory, and histopathologic
658 indicators of the development of progressive acute graft-versus-host disease. *J Invest Dermatol.* 1992;99(4):397-
659 402.
- 660 54. Lin J, Fan R, Zhao Z, Cummings OW, Chen S. Is the presence of 6 or fewer crypt apoptotic bodies sufficient for
661 diagnosis of graft versus host disease? A decade of experience at a single institution. *Am J Surg Pathol.*
662 2013;37(4):539-547.

663

664



C

Patient 1

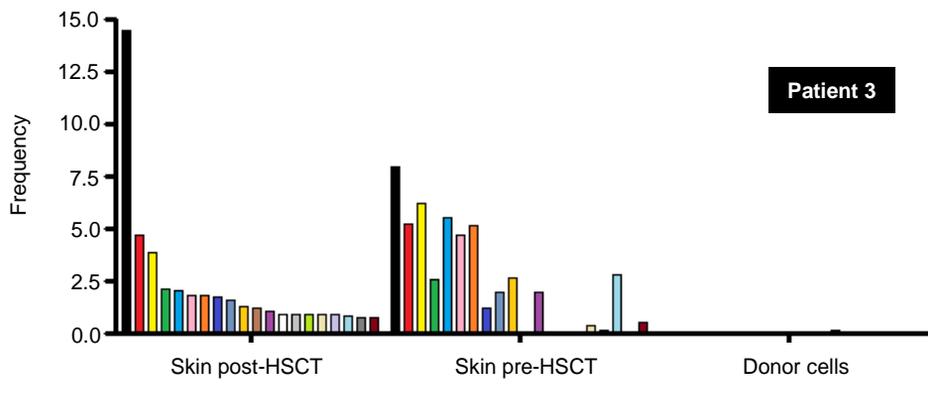
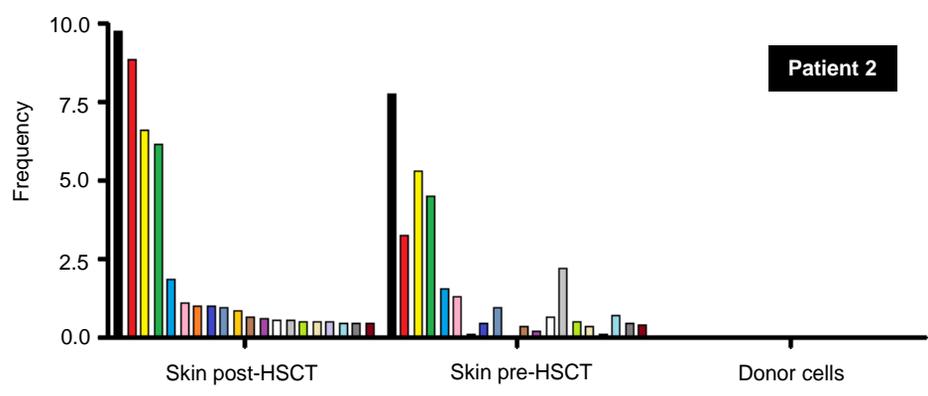
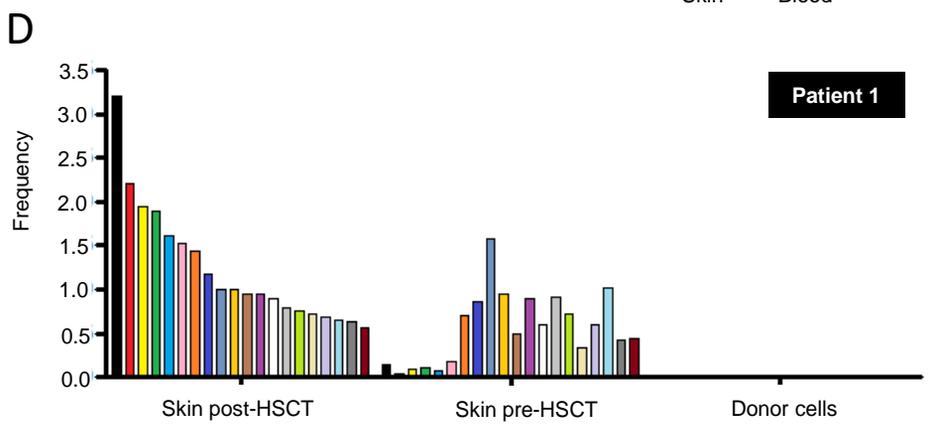
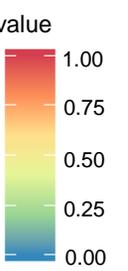
Donor cells	0			
Host blood post-HSCT	0.011	0.125		
Host blood pre-HSCT	0.035	0	0.307	
Host skin post-HSCT	0.831	0.001	0.009	0.009

Patient 2

Donor cells	0			
Host blood post-HSCT	0.001	0.074		
Host blood pre-HSCT	0.028	0	0.035	
Host skin post-HSCT	0.885	0.001	0.007	0.014

Patient 3

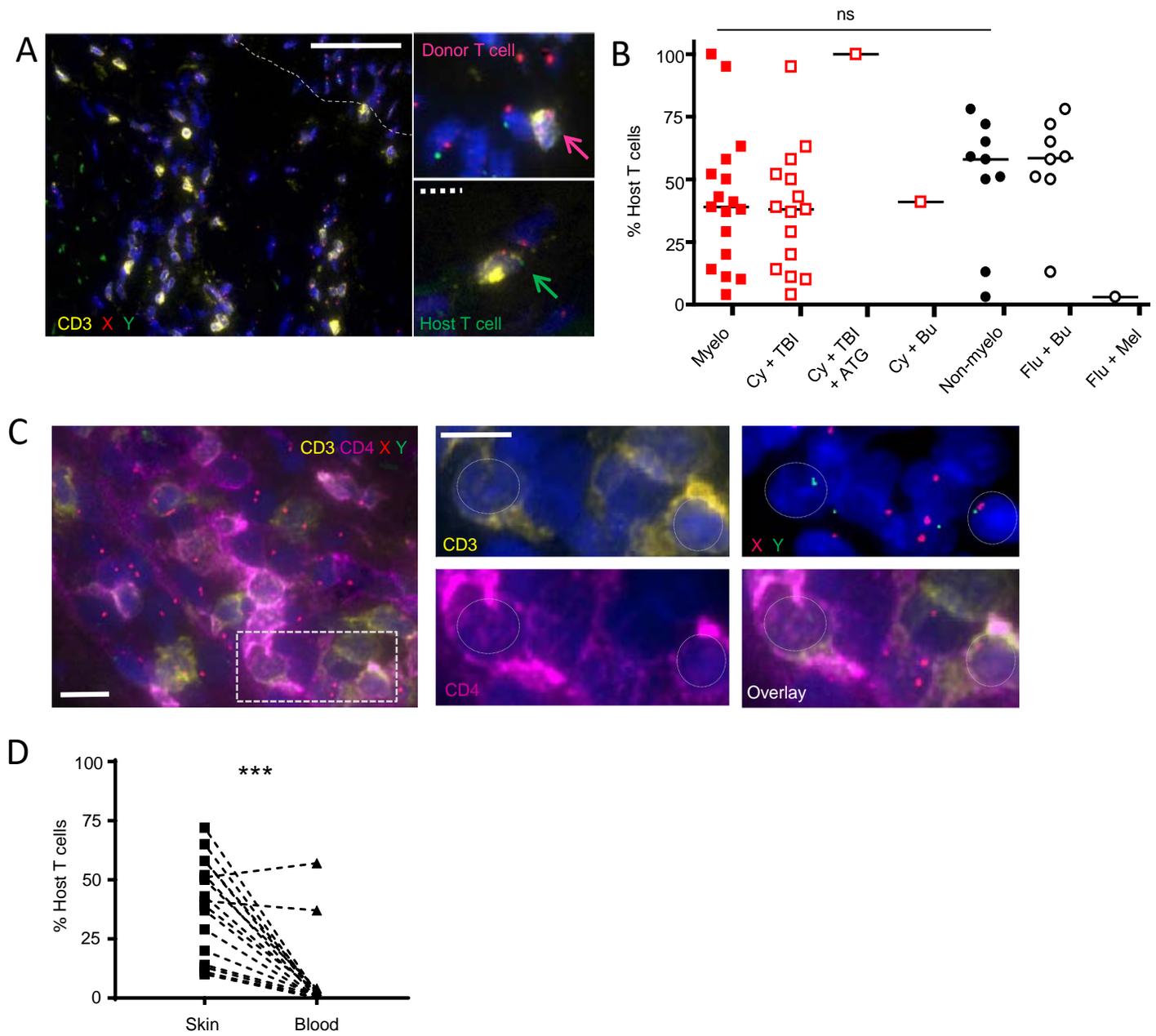
Donor cells	0			
Host blood post-HSCT	0.003	0.665		
Host blood pre-HSCT	0.026	0.001	0.024	
Host skin post-HSCT	0.774	0.003	0.021	0.021



662 **Figure 1. Host skin T cells survive HSCT conditioning.** (A) Example FISH-IF microscopy image of FFPE post-HSCT
663 skin showing: X chromosome, red; Y chromosome, green; CD3, yellow; DAPI nuclear stain, blue. White bar=10 μ m.
664 Green arrows point to Y chromosomes in host T cells. (B) Percent host T cell chimerism in skin and blood in paired
665 samples taken 30 \pm 6 days post-HSCT. Skin chimerism calculated via FISH-IF. Blood chimerism quantified via STR
666 analysis. (C) Heat map of Morisita overlap index for each patient (0, no similarity; 1, complete similarity). (D) Bar graph
667 for each patient showing the top 20 T cell clones in host skin post-HSCT and whether those same clones were present, and
668 if so at what frequency, in host skin pre-HSCT or donor infusion product (“Donor cells”). Each clone is color coded. (A-
669 D) N=3.

670

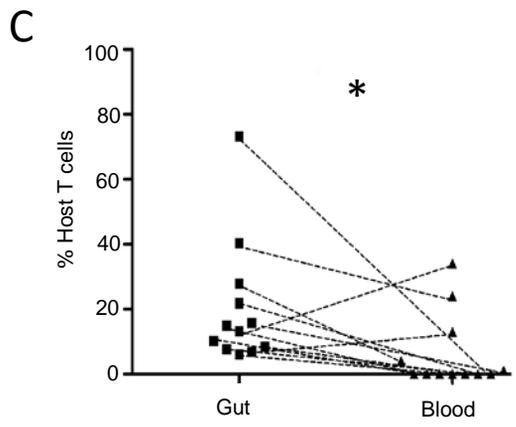
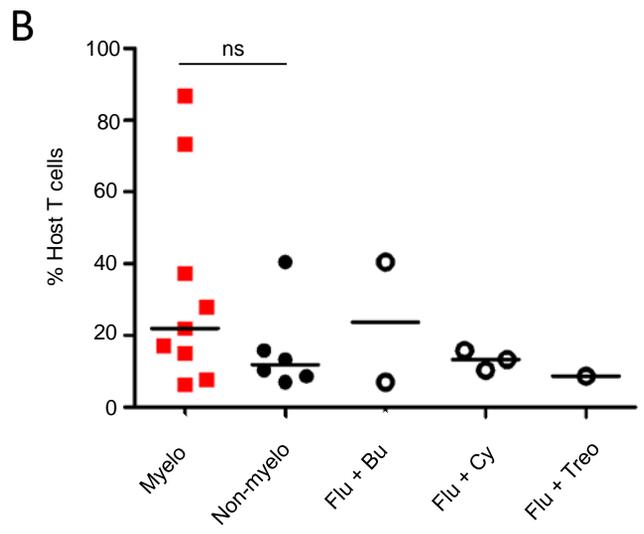
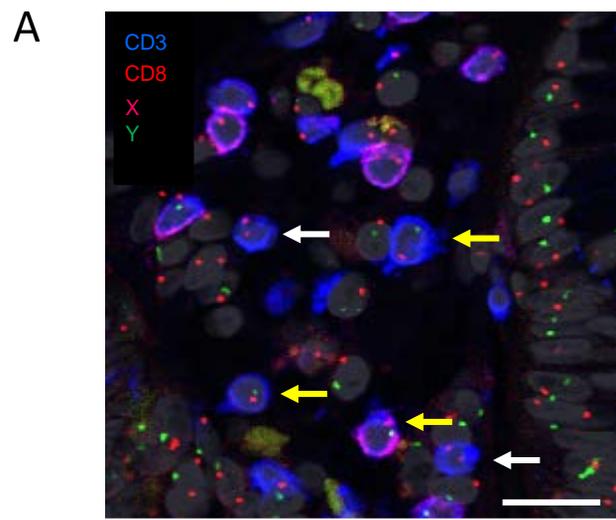
671



672 **Figure 2. Host T cells are present in skin during acute GVHD. (A)** Example FISH-IF from FFPE skin during acute
673 GVHD. X chromosome, red; Y chromosome, green; CD3, yellow; DAPI nuclear stain, blue. Solid white bar=50 μ m,
674 dotted white bar=10 μ m. Fine dotted line = dermal-epidermal junction. Pink arrow points to donor T cell; green arrow
675 points to host T cell. **(B)** Percent host T cell chimerism in skin during acute GVHD, determined by FISH-IF. Solid red
676 squares – all myeloablative-conditioned patients; Open red squares – breakdown of myeloablative patients by
677 conditioning regimen; Solid black circles – all non-myeloablative-conditioned patients; Open black circles – breakdown
678 of non-myeloablative patients by conditioning regimen. Black lines – median. Mann-Whitney test, two-tailed,
679 myeloablative vs non-myeloablative, $P=0.24$, not significant (ns). **(A,B)** $N=26$. **(C)** Example 5 color FISH-IF image from
680 FFPE skin during acute GVHD. X chromosome, red; Y chromosome, green; CD3, yellow; CD4, magenta; DAPI nuclear
681 stain, blue. Dotted white rectangle outlines region of enlarged images. White bars=10 μ m. Dotted gray circles outline
682 $CD3^+CD4^+$ host T cells. $N=5$ **(D)** Percent host T cell chimerism in skin, determined by FISH-IF, and blood, determined by
683 STR analysis, at the time of acute GVHD. $N=17$. Broken lines indicate paired specimens. Wilcoxon signed rank test, two-
684 tailed. *** $P<0.001$.

685

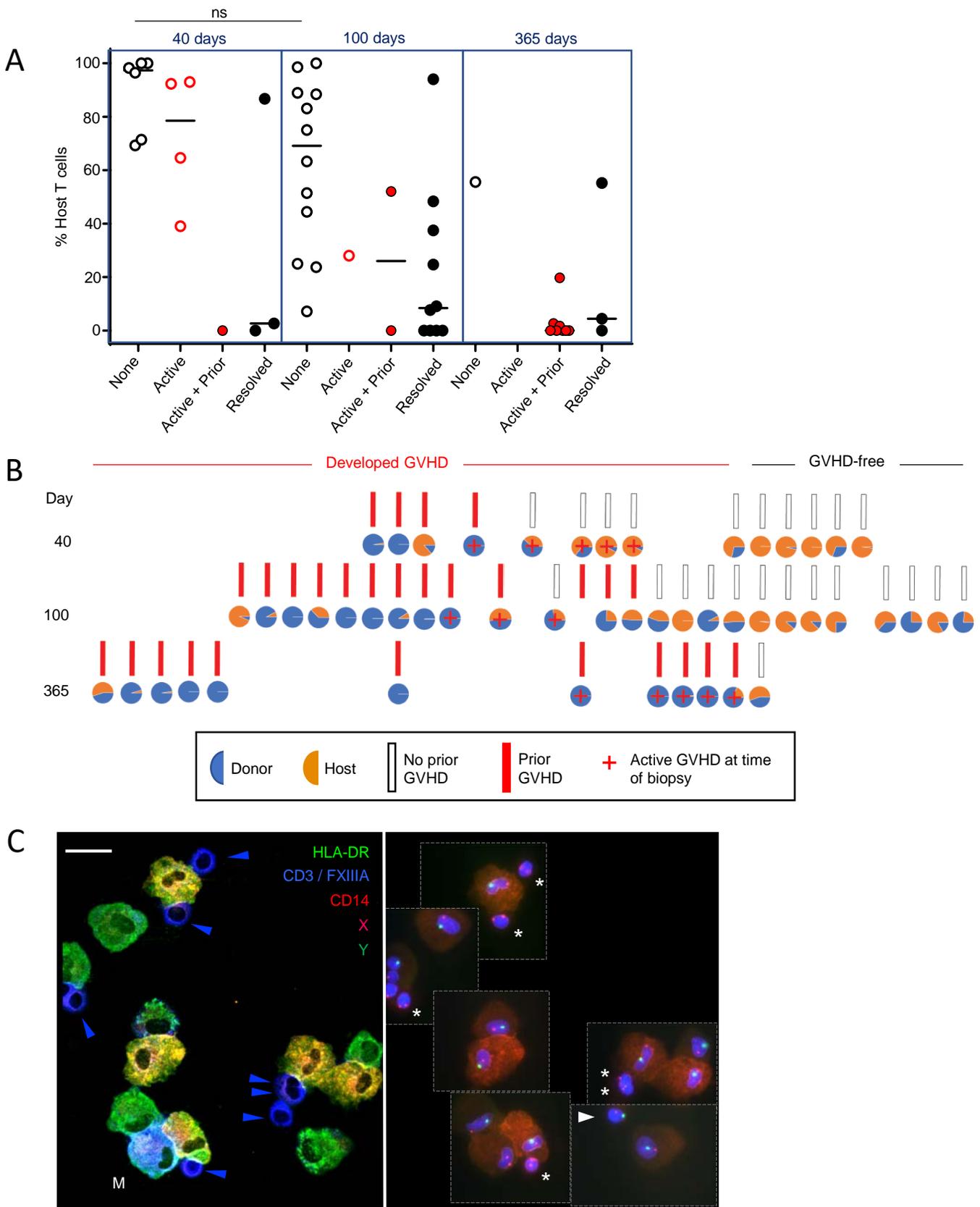
686



687 **Figure 3. Host T cells are present in gut during acute GVHD.** (A) Example FISH-IF from FFPE colon during acute
688 GVHD. X chromosome, red; Y chromosome, green; CD3, blue; CD8, red; Hoechst nuclear stain, grey. White bar=20 μ m.
689 Blue staining indicates CD4 T cells (CD3⁺CD8⁻) whereas pink staining (mixed blue and red) indicates CD3⁺CD8⁺ T cells.
690 White arrows point to donor (XX) T cells; yellow arrows point to recipient (XY) T cells. (B) Percent host gut T cell
691 chimerism in acute GVHD. Red squares – myeloablative-conditioned patients; Solid black circles - non-myeloablative-
692 conditioned patients; Open black circles - breakdown of non-myeloablative conditioning regimens. Black lines - median.
693 Mann-Whitney test, two-tailed, myeloablative vs non-myeloablative, P=0.27, not significant (ns). (A,B) N=15. (C)
694 Percent host gut T cell chimerism determined by FISH-IF versus peripheral blood chimerism determined by STR analysis.
695 N=12. Broken lines indicate paired samples. Wilcoxon signed rank test, two-tailed. *P=0.01.

696

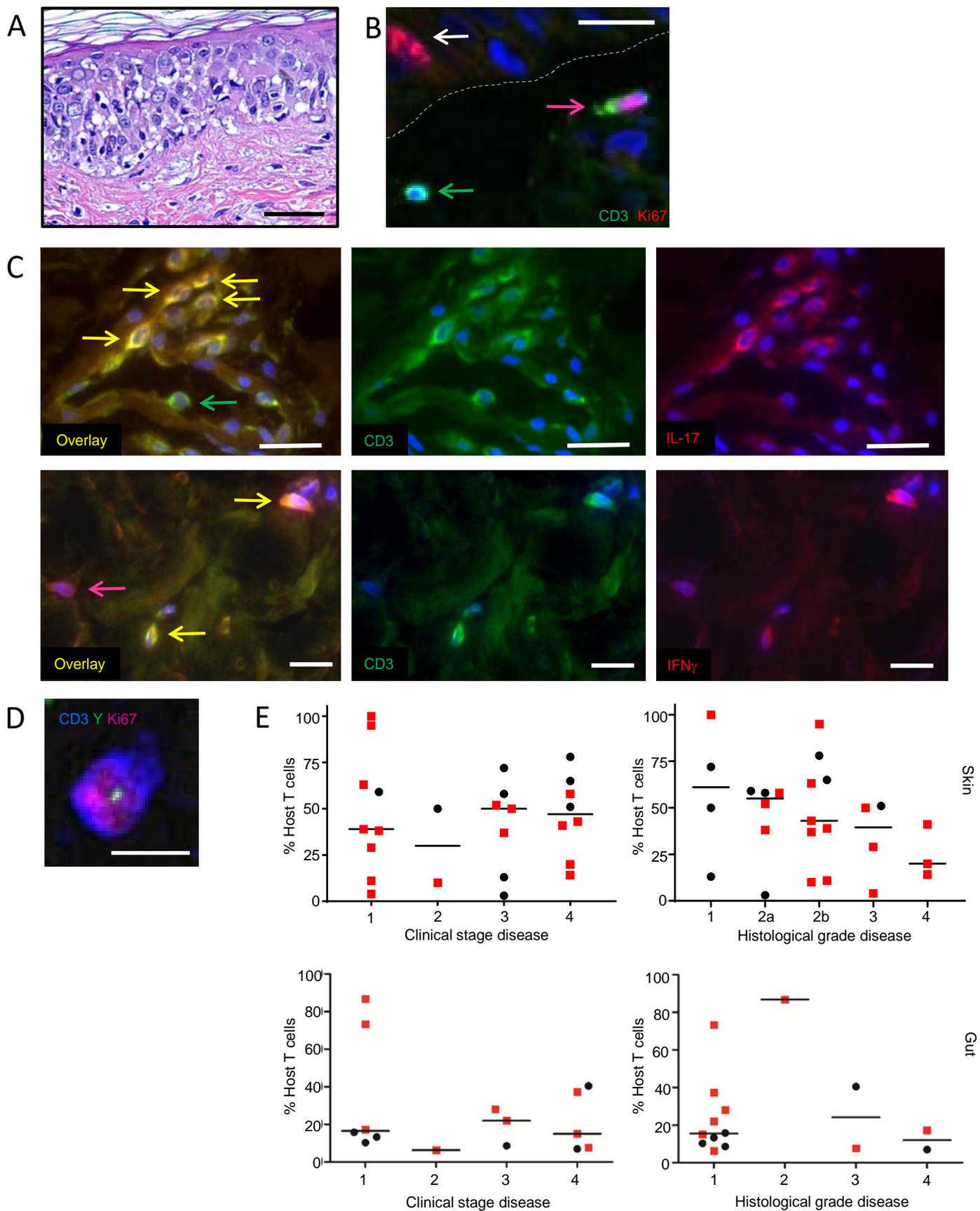
697



698 **Figure 4. Acute GVHD impacts host T cell chimerism in skin.** (A) Percent host T cell chimerism as quantified by
699 sequential FISH-IF on cytopins of skin migratory cells at 40, 100, and 365 days post-transplant. Open black circles – no
700 GVHD; Open red circles - active acute skin GVHD at time of biopsy; Closed red circles– active acute skin GVHD and
701 prior history of active acute skin GVHD; Closed black circles - history of acute skin GVHD resolved at time of biopsy.
702 Black lines – median. Dunn’s multiple comparison’s test for no GVHD 40 vs 100 days, $P>0.05$, not significant (B) FISH-
703 IF data of individual patients depicted in pie charts (gold – host; blue – donor) at 40, 100 and/or 365 days post-transplant.
704 Red plus sign indicates active acute skin GVHD at time of biopsy. Red bars indicate prior history of acute skin GVHD.
705 Clear bars indicate no prior history of acute skin GVHD. (C) Representative FISH-IF of a female patient transplanted with
706 a male donor, skin sample taken at 40 days post-transplant. This patient had prior history of acute skin GVHD resolved at
707 time of biopsy. Staining was performed for HLA-DR, green; CD14, red; CD3 and Factor XIIIa, both blue (easily
708 discernable by morphology), then FISH for X, pink and Y, green, chromosomes. Montages of corresponding FISH images
709 are outlined with gray dotted squares. Quantification yielded host T cell chimerism of 87% and myeloid cell (HLA-DR⁺
710 CD14⁺) cell chimerism of 98% donor. Asterisks indicate host (XX) T cells; white arrow points to donor (XY) T cell; blue
711 arrows point to CD3⁺ T cells; white M indicates macrophage. White bar=20 μ m. (A-C) N=34.

712

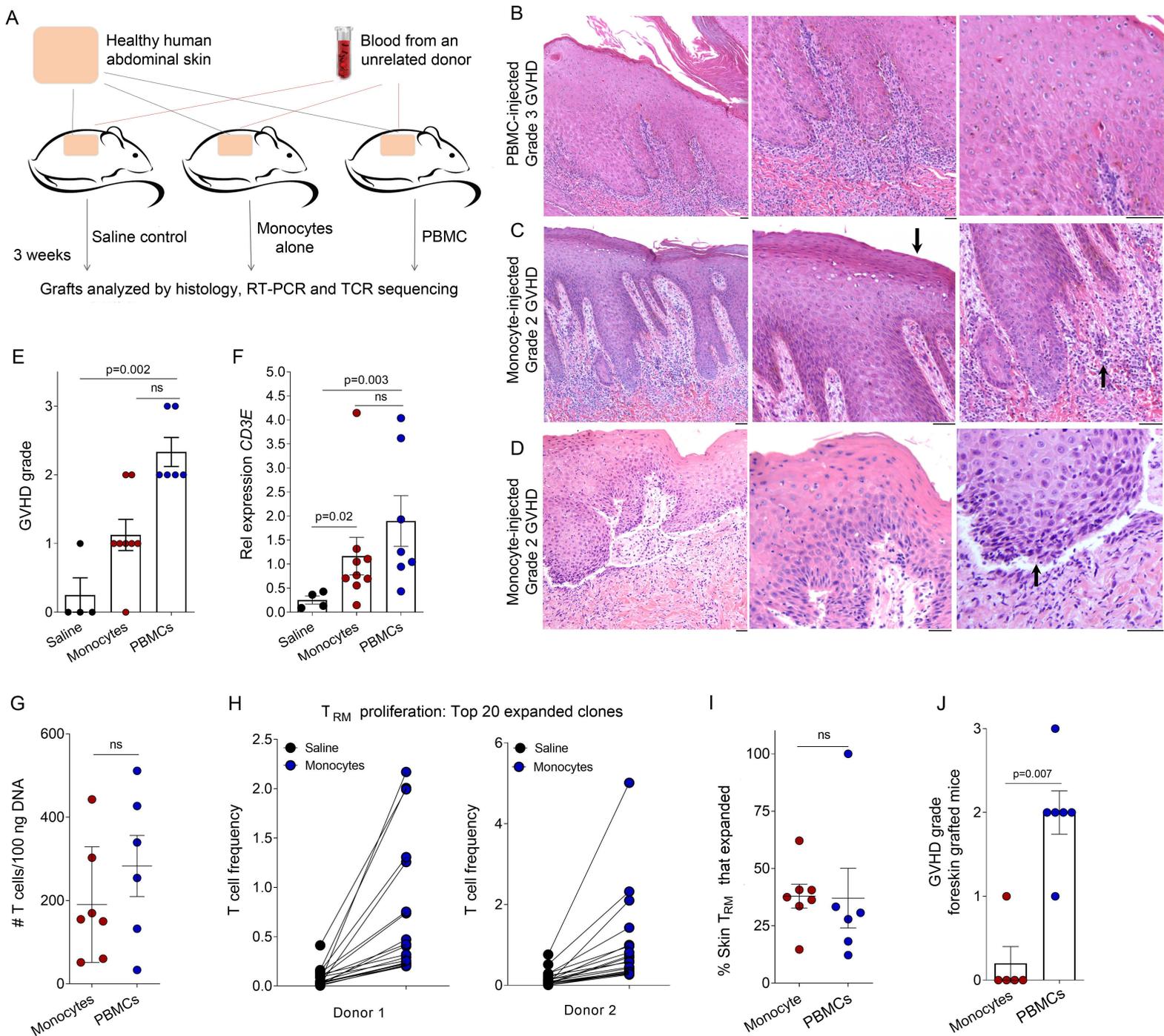
713



714 **Figure 5. Host T cells in skin and gut during acute GVHD are activated.** (A) Example H&E staining of skin from
715 patient with 100% host T cells. Black bar=50 μ m. (B) Example IF staining from same patient for CD3, green; Ki67, red;
716 Dapi nuclear stain, blue. Gray dotted line demarks dermal-epidermal junction. Pink arrow points to Ki67⁺CD3⁺ T cell;
717 green arrow points to Ki67⁻CD3⁺ T cell; white arrow points to Ki67⁺ keratinocyte. White bar=20 μ m. (C) Example IF
718 staining of same patient for CD3, green; pro-inflammatory cytokines, IFN γ or IL-17, red; DAPI nuclear stain, blue. White
719 bar=20 μ m. Yellow arrows point to cytokine producing CD3⁺ T cells; green arrow points to IL-17⁻CD3⁺ T cell; pink
720 arrow points to IFN γ ⁺CD3⁻ cell. (D) Example FISH-IF staining for Y chromosome, green; CD3, blue; Ki67, magenta;
721 Hoechst nuclear stain, grey. White bar=20 μ m. N=15. (E) Percent host T cells in skin during acute GVHD versus clinical
722 stage disease (left) and histologic grade (right). Skin, top row, N=26. Gut, bottom row, N=15. Red squares –
723 myeloablative-conditioned patients; Black circles – non-myeloablative-conditioned patients. Black lines – median.
724 Kruskal-Wallis test, skin and gut clinical stage and histological grade, not significant.

725

726



731 **Figure 6. Host skin T cells induce GVHD-like dermatitis independent of donor T cells in human skin grafted mice.**

732 (A) NSG mice were grafted with human skin, iv injected with saline, allogeneic monocytes alone, or allogeneic CD25-
733 depleted PBMC (labeled as PBMC); skin grafts were studied after three weeks. (B) Mice injected with PBMC developed
734 a GVHD-like dermatitis characterized by acanthosis, parakeratosis, dyskeratosis and lymphocytic infiltrates. (C)
735 Monocyte-injected mice developed similar changes, including lymphocytic infiltrates (left panel), epidermal acanthosis
736 and parakeratosis (middle panel), basal layer vacuolization and destruction of rete ridges (right panel). (D) A second
737 skin/blood pair with similar changes is shown. (B-D) Black bars=50 μ m. (E) Histologic grading of GVHD-like dermatitis
738 in skin grafts of monocyte- and PBMC-injected mice. (F-G) T cell numbers in skin, assessed by *CD3E* gene expression
739 (F) and by HTS (G), were similar in monocyte- and PBMC-injected mice. (H) Host skin-resident T cells (T_{RM}) proliferate
740 after exposure to donor monocytes. The frequencies of the 20 most frequent T cell clones found in grafts from both saline-
741 and monocyte-injected mice are shown. (I) Similar percentages of T_{RM} clones proliferated in monocyte- and PBMC-
742 injected mice. Histology and transcript analysis performed on saline-injected (n=4), monocyte-injected (n=9) and PBMC-
743 injected (n=7) mice. Clonality performed on monocyte-injected (n=7) and PBMC-injected (n=6) mice. (J) GVHD did not
744 develop in the absence of host skin T cells. Mice grafted with human foreskin, which contains APC but lacks T cells, and
745 infused with PBMC (n=6) developed GVHD-like dermatitis but monocyte-injected (n=5) mice did not. Mean and SEM
746 (error bars) are shown. Differences between two independent groups were detected using Mann–Whitney test, one-tailed.
747 One-way Kruskal–Wallis test with Dunn’s post-test was used for comparing multiple independent groups.